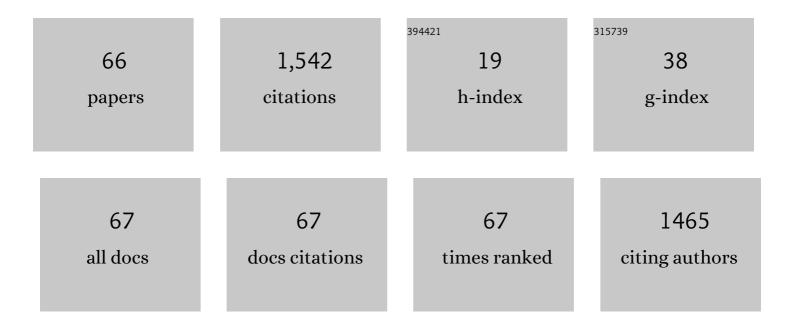
Kevin L Schulte

List of Publications by Year in descending order

Source: https://exaly.com/author-pdf/9227644/publications.pdf Version: 2024-02-01



| # | Article | IF | CITATIONS |
|----|---|------|-----------|
| 1 | (110)-Oriented GaAs Devices and Spalling as a Platform for Low-Cost III-V Photovoltaics. IEEE Journal of Photovoltaics, 2022, 12, 962-967. | 2.5 | 2 |
| 2 | Thermophotovoltaic efficiency of 40%. Nature, 2022, 604, 287-291. | 27.8 | 108 |
| 3 | Compositionally graded Ga1â^'xInxP buffers grown by static and dynamic hydride vapor phase epitaxy at rates up to 1 <i>I¼</i> m/min. Applied Physics Letters, 2021, 118, . | 3.3 | 4 |
| 4 | Recent HVPE grown solar cells at NREL. , 2021, , . | | 2 |
| 5 | Control of Surface Morphology during the Growth of (110)-Oriented GaAs by Hydride Vapor Phase Epitaxy. Crystal Growth and Design, 2021, 21, 3916-3921. | 3.0 | 3 |
| 6 | (110)-Oriented GaAs Devices and Spalling as a Platform for Low-Cost III-V Photovoltaics. , 2021, , . | | 2 |
| 7 | Effect of Doping Density on the Performance of Metamorphic GaInAs Solar Cells Grown by Dynamic Hydride Vapor Phase Epitaxy. , 2021, , . | | 0 |
| 8 | Inverted metamorphic GalnAs solar cell grown by dynamic hydride vapor phase epitaxy. Applied Physics Letters, 2021, 119, . | 3.3 | 4 |
| 9 | Surface chemistry models for GaAs epitaxial growth and hydride cracking using reacting flow simulations. Journal of Applied Physics, 2021, 130, 115702. | 2.5 | 1 |
| 10 | Dopant Diffusion Control for Improved Tandem Cells Grown by D-HVPE. IEEE Journal of Photovoltaics, 2021, 11, 1251-1255. | 2.5 | 3 |
| 11 | Guided Optimization of Phase-Unstable III–V Compositionally Graded Buffers by Cathodoluminescence Spectrum Imaging. IEEE Journal of Photovoltaics, 2020, 10, 109-116. | 2.5 | 7 |
| 12 | Inverted metamorphic AlGaInAs/GaInAs tandem thermophotovoltaic cell designed for thermal energy grid storage application. Journal of Applied Physics, 2020, 128, . | 2.5 | 10 |
| 13 | Effect of hydride vapor phase epitaxy growth conditions on the degree of atomic ordering in GaInP. Journal of Applied Physics, 2020, 128, . | 2.5 | 3 |
| 14 | GaAs growth rates of 528 μ m/h using dynamic-hydride vapor phase epitaxy with a nitrogen carrier gas. Applied Physics Letters, 2020, 116, . | 3.3 | 14 |
| 15 | Six-junction III–V solar cells with 47.1% conversion efficiency under 143 Suns concentration. Nature Energy, 2020, 5, 326-335. | 39.5 | 408 |
| 16 | GaAs Solar Cell Grown by Dynamic Hydride Vapor Phase Epitaxy Using Nitrogen Carrier Gas. , 2020, , . | | 0 |
| 17 | Improved contacts for tandem cells with enhanced effciency grown by D-HVPE. , 2020, , . | | 0 |
| 18 | Gallium arsenide solar cells grown at rates exceeding 300 µm hâ^'1 by hydride vapor phase epitaxy. Nature Communications, 2019, 10, 3361. | 12.8 | 61 |

KEVIN L SCHULTE

| # | Article | IF | CITATIONS |
|----|--|------|-----------|
| 19 | Germanium-on-Nothing for Epitaxial Liftoff of GaAs Solar Cells. Joule, 2019, 3, 1782-1793. | 24.0 | 41 |
| 20 | Carrier-Transport Study of Gallium Arsenide Hillock Defects. Microscopy and Microanalysis, 2019, 25, 1160-1166. | 0.4 | 4 |
| 21 | III-V-Based Optoelectronics with Low-Cost Dynamic Hydride Vapor Phase Epitaxy. Crystals, 2019, 9, 3. | 2.2 | 42 |
| 22 | Uniformity of GaAs solar cells grown in a kinetically-limited regime by dynamic hydride vapor phase epitaxy. Solar Energy Materials and Solar Cells, 2019, 197, 84-92. | 6.2 | 7 |
| 23 | Toward Low-Cost 4-Terminal GaAs//Si Tandem Solar Cells. ACS Applied Energy Materials, 2019, 2, 2375-2380. | 5.1 | 17 |
| 24 | Fabrication of Thin III-V Solar Cells on Ni Films using Electroless Ni Deposition. , 2019, , . | | 0 |
| 25 | Analysis of GaAs Solar Cells Grown on 50 mm Wafers at 700 °C by Dynamic Hydride Vapor Phase Epitaxy. , 2019, , . | | 0 |
| 26 | High Performance GaAs Solar Cells Grown at High Growth Rates by Atmospheric-Pressure Dynamic Hydride Vapor Phase Epitaxy. , 2019, , . | | 0 |
| 27 | Growth of AlGaAs, AlInP, and AlGaInP by Hydride Vapor Phase Epitaxy. ACS Applied Energy Materials, 2019, 2, 8405-8410. | 5.1 | 19 |
| 28 | Internal Resistive Barriers Related to Zinc Diffusion During the Growth of Inverted Metamorphic Multijunction Solar Cells. IEEE Journal of Photovoltaics, 2019, 9, 167-173. | 2.5 | 14 |
| 29 | Building a Six-Junction Inverted Metamorphic Concentrator Solar Cell. IEEE Journal of Photovoltaics, 2018, 8, 626-632. | 2.5 | 148 |
| 30 | Increased fracture depth range in controlled spalling of (100)-oriented germanium via electroplating. Thin Solid Films, 2018, 649, 154-159. | 1.8 | 13 |
| 31 | High-efficiency inverted metamorphic 1.7/1.1 eV GaInAsP/GaInAs dual-junction solar cells. Applied Physics Letters, 2018, 112, . | 3.3 | 47 |
| 32 | High growth rate hydride vapor phase epitaxy at low temperature through use of uncracked hydrides. Applied Physics Letters, 2018, 112, . | 3.3 | 22 |
| 33 | Tunnel Junction Development Using Hydride Vapor Phase Epitaxy. IEEE Journal of Photovoltaics, 2018, 8, 322-326. | 2.5 | 13 |
| 34 | GaAs Solar Cells Grown on Unpolished, Spalled Ge Substrates. , 2018, , . | | 4 |
| 35 | Improvement of Short-Circuit Current Density in GaInP Solar Cells Grown by Dynamic Hydride Vapor Phase Epitaxy. IEEE Journal of Photovoltaics, 2018, 8, 1616-1620. | 2.5 | 8 |
| 36 | Six-junction concentrator solar cells. AIP Conference Proceedings, 2018, , . | 0.4 | 21 |

KEVIN L SCHULTE

| # | Article | IF | CITATIONS |
|----|---|-----|-----------|
| 37 | Tunable Bandgap GaInAsP Solar Cells With 18.7% Photoconversion Efficiency Synthesized by Low-Cost and High-Growth Rate Hydride Vapor Phase Epitaxy. IEEE Journal of Photovoltaics, 2018, 8, 1577-1583. | 2.5 | 13 |
| 38 | Strategies for Thinning Graded Buffer Regions in Metamorphic Solar Cells and Performance Tradeoffs. IEEE Journal of Photovoltaics, 2018, 8, 1349-1354. | 2.5 | 4 |
| 39 | III–V Solar Cells Grown on Unpolished and Reusable Spalled Ge Substrates. IEEE Journal of Photovoltaics, 2018, 8, 1384-1389. | 2.5 | 11 |
| 40 | Multijunction Ga _{0.5} In _{0.5} P/GaAs solar cells grown by dynamic hydride vapor phase epitaxy. Progress in Photovoltaics: Research and Applications, 2018, 26, 887-893. | 8.1 | 33 |
| 41 | Development of GaInP Solar Cells Grown by Hydride Vapor Phase Epitaxy. IEEE Journal of Photovoltaics, 2017, 7, 1153-1158. | 2.5 | 23 |
| 42 | Near-field transport imaging applied to photovoltaic materials. Solar Energy, 2017, 153, 134-141. | 6.1 | 9 |
| 43 | Pathway to 50% efficient inverted metamorphic concentrator solar cells. AIP Conference Proceedings, 2017, , . | 0.4 | 15 |
| 44 | Highly Transparent Compositionally Graded Buffers for New Metamorphic Multijunction Solar Cell Designs. IEEE Journal of Photovoltaics, 2017, 7, 347-353. | 2.5 | 19 |
| 45 | Reduced dislocation density in GaxIn1â^'xP compositionally graded buffer layers through engineered glide plane switch. Journal of Crystal Growth, 2017, 464, 20-27. | 1.5 | 10 |
| 46 | Upright and Inverted Single-Junction GaAs Solar Cells Grown by Hydride Vapor Phase Epitaxy. IEEE Journal of Photovoltaics, 2017, 7, 157-161. | 2.5 | 36 |
| 47 | Notice of Removal Upright and inverted single junction GaAs solar cells grown by hydride vapor phase epitaxy. , 2017, , . | | 1 |
| 48 | Analysis of GaInP Solar Cells Grown by Hydride Vapor Phase Epitaxy. , 2017, , . | | 0 |
| 49 | Notice of Removal Highly transparent compositionally graded buffers for new metamorphic multi-junction solar cell designs. , 2017, , . | | 0 |
| 50 | GaLnAsP Solar Cells Grown by Hydride Vapor Phase Epitaxy for One-Sun & Low-Concentration III-V/Si Photovoltaics. , 2017, , . | | 0 |
| 51 | Controlled exfoliation of (100) GaAs-based devices by spalling fracture. Applied Physics Letters, 2016, 108, . | 3.3 | 60 |
| 52 | InGaAsP solar cells grown by hydride vapor phase epitaxy. , 2016, , . | | 6 |
| 53 | A kinetic model for GaAs growth by hydride vapor phase epitaxy. , 2016, , . | | 4 |
| 54 | Enhanced Incorporation of P into Tensile-Strained GaAs1-yPyLayers Grown by Metal-Organic Vapor Phase Epitaxy at Very Low Temperatures. ECS Journal of Solid State Science and Technology, 2016, 5, P183-P189. | 1.8 | 3 |

KEVIN L SCHULTE

| # | Article | IF | CITATIONS |
|----|--|------|-----------|
| 55 | Computational fluid dynamics-aided analysis of a hydride vapor phase epitaxy reactor. Journal of Crystal Growth, 2016, 434, 138-147. | 1.5 | 26 |
| 56 | GaAs Solar Cells Grown by Hydride Vapor-Phase Epitaxy and the Development of GaInP Cladding Layers. IEEE Journal of Photovoltaics, 2016, 6, 191-195. | 2.5 | 37 |
| 57 | Low cost GaAs solar cells grown by hydride vapor phase epitaxy and the development of GaInP cladding layers. , 2015, , . | | 4 |
| 58 | Modeling of gas curtains in a dual chamber hydride vapor phase epitaxial photovoltaic growth reactor. , 2015, , . | | 3 |
| 59 | Evolution of epilayer tilt in thick In Ga1â^'As metamorphic buffer layers grown by hydride vapor phase epitaxy. Journal of Crystal Growth, 2015, 426, 283-286. | 1.5 | 5 |
| 60 | A model for arsenic anti-site incorporation in GaAs grown by hydride vapor phase epitaxy. Journal of Applied Physics, 2014, 116, . | 2.5 | 8 |
| 61 | Lowâ€strain, quantumâ€cascadeâ€laser active regions grown on metamorphic buffer layers for emission in the 3.0–4.0 μm wavelength region. IET Optoelectronics, 2014, 8, 25-32. | 3.3 | 7 |
| 62 | Planarization and Processing of Metamorphic Buffer Layers Grown by Hydride Vapor-Phase Epitaxy. Journal of Electronic Materials, 2014, 43, 873-878. | 2.2 | 2 |
| 63 | Metalorganic vapor phase growth of quantum well structures on thick metamorphic buffer layers grown by hydride vapor phase epitaxy. Journal of Crystal Growth, 2013, 370, 293-298. | 1.5 | 19 |
| 64 | Heteroepitaxy of GaAs on (001) ⇒ 6° Ge substrates at high growth rates by hydride vapor phase epitaxy. Journal of Applied Physics, 2013, 113, 174903. | 2.5 | 8 |
| 65 | Controlled formation of GaAs pn junctions during hydride vapor phase epitaxy of GaAs. Journal of Crystal Growth, 2012, 352, 253-257. | 1.5 | 24 |
| 66 | Effect of crystal phase composition on the reductive and oxidative abilities of TiO2 nanotubes under UV and visible light. Applied Catalysis B: Environmental, 2010, 97, 354-360. | 20.2 | 100 |